

(Chalcone Project)

David Behrle

INTRODUCTION

Malaria remains a major public health issue with nearly 230 million cases estimated worldwide in 2019, the vast majority of which were reported in Africa owing to infection by protozoan parasites in the genus *Plasmodium*, most notably *Plasmodium falciparum*.¹ Historically, chloroquine and its derivatives have been used to treat malaria however, the emergence of chloroquine-resistant strains of *P. falciparum* has greatly decreased the efficacy of these treatments creating an urgent need for alternative antimalarial compounds.^{1,2} Chalcones are a class of α,β -unsaturated ketones belonging to the flavonoid family which remain of significant interest due to their relatively simple synthetic chemistry and diverse application as scaffolds in medicinal chemistry.³ Discovery of the antimalarial activity of the naturally occurring chalcone Licochalcone A, originally isolated from Chinese licorice roots, has prompted research into chalcones and chalcone hybrids as antimalarial candidates.^{4,5} Hybridization has been explored as a method for overcoming drug resistance in *P. falciparum*, this is supported by the observation that many chloroquine derivatives and analogs retain activity against chloroquine-resistant strains of *P. falciparum*.^{4,6} Chloroquine-chalcone based hybrids have been shown to have potent antimalarial activity against chloroquine-resistant *P. falciparum* in vitro when compared with chloroquine.⁶ Likewise, triazole linked chalcones, ferrocenyl chalcones, and caffeine based chalcones among others have been evaluated as potential antimalarial, antitrypanosomal, antileishmanial, and antiplasmodial agents.^{3,7,8} Structure-activity relationship studies of various chalcone derivatives have shown that different structural requirements exist for antimalarial and antileishmanial activity respectively, with the A ring being more significant in antileishmanial activity compared with antimalarial activity in which both A and B rings are important.⁹ Stereoisomerism has also been shown to have an effect on the antimalarial activity of chalcone derivatives. Synthesis and evaluation of conformationally restricted derivatives of known antiplasmodial chalcones has demonstrated that Z-locked chalcone derivatives are effectively inactive while E-locked analogs show equivalent activity and potency to the parent chalcone.¹⁰ Chalcone derivatives lacking the α,β -unsaturated ketone bridge exhibit significantly less antimalarial activity, with saturated analogs showing a 10-fold decrease in antimalarial activity.¹¹

METHODS AND RESULTS

Instrumentation. Nuclear magnetic resonance (NMR) spectra were recorded on a Bruker Ultrashield™ (CDCl₃, 400 MHz) calibrated using deuterated solvent (CDCl₃: ¹H NMR: 7.26 ppm). IR spectra were recorded on a Nicolet Summit™ FTIR spectrometer. UV-Vis spectra were recorded on a Vernier Fluorescence/UV-Vis spectrophotometer.

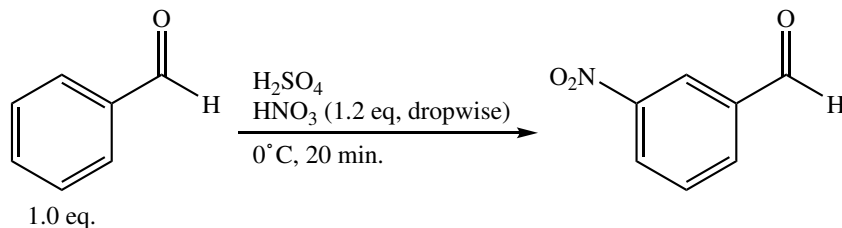


Figure 1: Nitration of benzaldehyde

Procedure. Benzaldehyde (10.4 g, 98.0 mmol) was added to a 250 mL round bottom flask and cooled to 0°C , followed by addition of sulfuric acid (30 mL). To this solution, nitric acid (7 mL) was added dropwise over 10 minutes, and allowed to stir for 10 minutes. Reaction progress was monitored with TLC (9:1 hexanes:EtOAc). When the reaction was complete, the reaction mixture was quenched with ice (~50 mL), the crude product was filtered by vacuum, and recrystallized from isopropanol.

3-nitrobenzaldehyde: yellow crystals. Hexanes:EtOAc 9:1 $R_f = 0.43$. $^1\text{H-NMR}$ (400 MHz, CDCl_3): δ 7.761 - 7.801 (t, 1H), 8.236 - 8.256 (d, 1H), 8.487 - 8.516 (dq, 1H), 8.728 (s, 1H), 10.134 (s, 1H). **IR** (neat): 3069, 2981, 2884, 1698, 1523, 1348, 1198 cm^{-1} **UV-Vis:** $\lambda_{\text{max}} = 220 \text{ nm}$. **MP:** 47.6°C . **Yield:** (7.901 g, 53.35%).

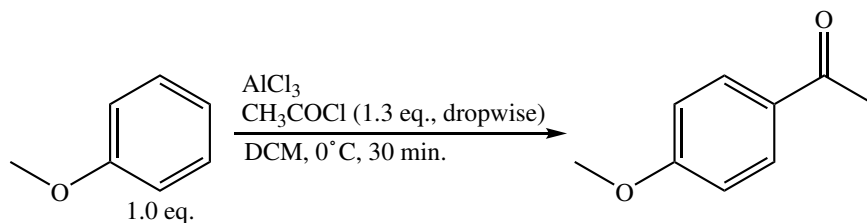


Figure 2: Acetylation of anisole

Procedure. Aluminum chloride (14 g) in DCM (15.0 mL) was added to a 250 mL two-necked round bottom flask and cooled to 0°C , followed by dropwise addition of acetyl chloride (9.27 g, 118 mmol) in DCM (10.0 mL) over 10 minutes with magnetic stirring. To the resulting mixture was added anisole (10.0 g, 93.9 mmol) dropwise over 30 minutes. Reaction progress was monitored using TLC (9:1 hexanes:EtOAc). When the reaction was completed, the reaction mixture was quenched in a beaker containing ice (~30 mL) and hydrochloric acid (10 mL), then neutralized with saturated sodium bicarbonate. The resulting mixture was extracted with saturated sodium bicarbonate (2x1 vol.), washed with brine (1 vol.), dried with anhydrous sodium sulfate, and the solvent was evaporated under reduced pressure.

4-methoxyacetophenone: Colorless solid/pale yellow liquid. Hexanes:EtOAc 9:1 $R_f = 0.53$. $^1\text{H-NMR}$ (400 MHz): δ 2.539 (s, 3H), 3.849 (s, 3H), 6.907 - 6.929 (d, 2H) 7.912 - 7.934 (d, 2H). **IR** (neat): 2970, 2842, 1671, 1597, 1509, 1417, 1357, 1247, 1169, 1025, 956, 832 cm^{-1} . **UV-Vis:** $\lambda_{\text{max}} = 270 \text{ nm}$. **Yield:** (9.247 g, 66.24%).

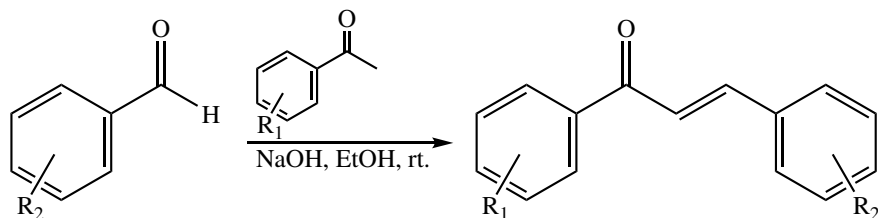


Figure 3: Aldol condensation of benzaldehyde and acetophenone

Prodedure. To a 150 mL Erlenmeyer flask was added 3-nitrobenzaldehyde (0.76 g, 5.0 mmol) followed by the acetophenone (5.0 mmol) and 95% EtOH (4 mL). Once all the solid was dissolved, NaOH solution (0.5 mL) was added with constant stirring until the mixture solidified. After 5 minutes of additional stirring, the resulting solid was quenched with ice water (~10 mL), filtered by vacuum, and recrystallized from hot 95% EtOH.

3-(3-nitrophenyl)-1-phenylprop-2-en-1-one: light green powder. $^1\text{H-NMR}$ (400 MHz): δ 7.527 - 7.564 (t, 2H), 7.608 - 7.644 (t, 2H), 7.648 - 7.684 (d, 1H), 7.823 - 7.863 (d, 1H), 7.922 - 7.941 (d, 1H), 8.043 - 8.067 (d, 2H), 8.259 - 8.282 (dq, 1H), 8.519 - 8.528 (t, 1H). **IR** (neat): 3071, 1659, 1606, 1526, 1446, 1349, 1217 cm^{-1} . **UV-Vis:** $\lambda_{\text{max}} = 237 \text{ nm}$. **Yield:** (1.989 g, 158.3%)

1-(4-methoxyphenyl)-3-(3-nitrophenyl)prop-2-en-1-one: blue-green powder. $^1\text{H-NMR}$ (400 MHz): δ 3.914 (s, 3H), 7.005 - 7.027 (d, 2H), 7.596 - 7.636 (t, 1H), 7.648 - 7.687 (d, 1H), 7.806 - 7.846 (d, 1H), 7.906 - 7.925 (d, 1H), 8.061 - 8.083 (d, 2H), 8.239 - 8.268 (dq, 1H), 8.515 - 8.524 (t, 1H). **IR** (neat): 3357, 2981, 2888, 1662, 1595, 1521, 1339, 1258, 1167 cm^{-1} . **UV-Vis:** $\lambda_{\text{max}} = 322 \text{ nm}$. **Yield:** (847 mg, 59.92%)

REFERENCES

- [1] Fikadu, M.; Ashenafi, E. Malaria: An Overview. *Infection and Drug Resistance* **2023**, Volume 16, 3339–3347, DOI: 10.2147/idr.s405668.
- [2] Yadav, N.; Dixit, S. K.; Bhattacharya, A.; Mishra, L. C.; Sharma, M.; Awasthi, S. K.; Bhasin, V. K. Antimalarial Activity of Newly Synthesized Chalcone Derivatives In Vitro. *Chemical Biology & Drug Design* **2012**, 80, 340–347, DOI: 10.1111/j.1747-0285.2012.01383.x.
- [3] Qin, H.-L.; Zhang, Z.-W.; Lekkala, R.; Alsulami, H.; Rakesh, K. Chalcone hybrids as privileged scaffolds in antimalarial drug discovery: A key review. *European Journal of Medicinal Chemistry* **2020**, 193, 112215, DOI: 10.1016/j.ejmech.2020.112215.
- [4] Cheng, P.; Yang, L.; Huang, X.; Wang, X.; Gong, M. Chalcone hybrids and their antimalarial activity. *Archiv der Pharmazie* **2020**, 353, DOI: 10.1002/ardp.201900350.
- [5] Chen, M.; Theander, T. G.; Christensen, S. B.; Hviid, L.; Zhai, L.; Kharazmi, A. Licochalcone A, a new antimalarial agent, inhibits in vitro growth of the human malaria parasite *Plasmodium falciparum* and protects mice from *P. yoelii* infection. *Antimicrobial Agents and Chemotherapy* **1994**, 38, 1470–1475, DOI: 10.1128/aac.38.7.1470.
- [6] Sashidhara, K. V.; Avula, S. R.; Palnati, G. R.; Singh, S. V.; Srivastava, K.; Puri, S. K.; Saxena, J. Synthesis and in vitro evaluation of new chloroquine-chalcone hybrids against chloroquine-resistant strain of *Plasmodium falciparum*. *Bioorganic & Medicinal Chemistry Letters* **2012**, 22, 5455–5459, DOI: 10.1016/j.bmcl.2012.07.028.
- [7] Singh, A.; Gut, J.; Rosenthal, P. J.; Kumar, V. 4-Aminoquinoline-ferrocenyl-chalcone conjugates: Synthesis and anti-plasmodial evaluation. *European Journal of Medicinal Chemistry* **2017**, 125, 269–277, DOI: 10.1016/j.ejmech.2016.09.044.
- [8] Insuasty, B.; Ramírez, J.; Becerra, D.; Echeverry, C.; Quiroga, J.; Abonia, R.; Robledo, S. M.; Vélez, I. D.; Upegui, Y.; Muñoz, J. A.; Ospina, V.; Nogueras, M.; Cobo, J. An efficient synthesis of new caffeine-based chalcones, pyrazolines and pyrazolo[3, 4-b][1, 4]diazepines as potential antimalarial, antitrypanosomal and antileishmanial agents. *European Journal of Medicinal Chemistry* **2015**, 93, 401–413, DOI: 10.1016/j.ejmech.2015.02.040.
- [9] Liu, M.; Wilairat, P.; Croft, S. L.; Tan, A. L.-C.; Go, M.-L. Structure–activity relationships of antileishmanial and antimalarial chalcones. *Bioorganic & Medicinal Chemistry* **2003**, 11, 2729–2738, DOI: 10.1016/s0968-0896(03)00233-5.
- [10] Larsen, M.; Kromann, H.; Kharazmi, A.; Nielsen, S. F. Conformationally restricted anti-plasmodial chalcones. *Bioorganic & Medicinal Chemistry Letters* **2005**, 15, 4858–4861, DOI: 10.1016/j.bmcl.2005.07.012.

- [11] Li, R.; Kenyon, G. L.; Cohen, F. E.; Chen, X.; Gong, B.; Dominguez, J. N.; Davidson, E.; Kurzban, G.; Miller, R. E.; Nuzum, E. O.; Rosenthal, P. J.; McKerrow, J. H. In Vitro Antimalarial Activity of Chalcones and Their Derivatives. *Journal of Medicinal Chemistry* **1995**, *38*, 5031–5037, DOI: 10.1021/jm00026a010.

APPENDIX A: SPECTRA

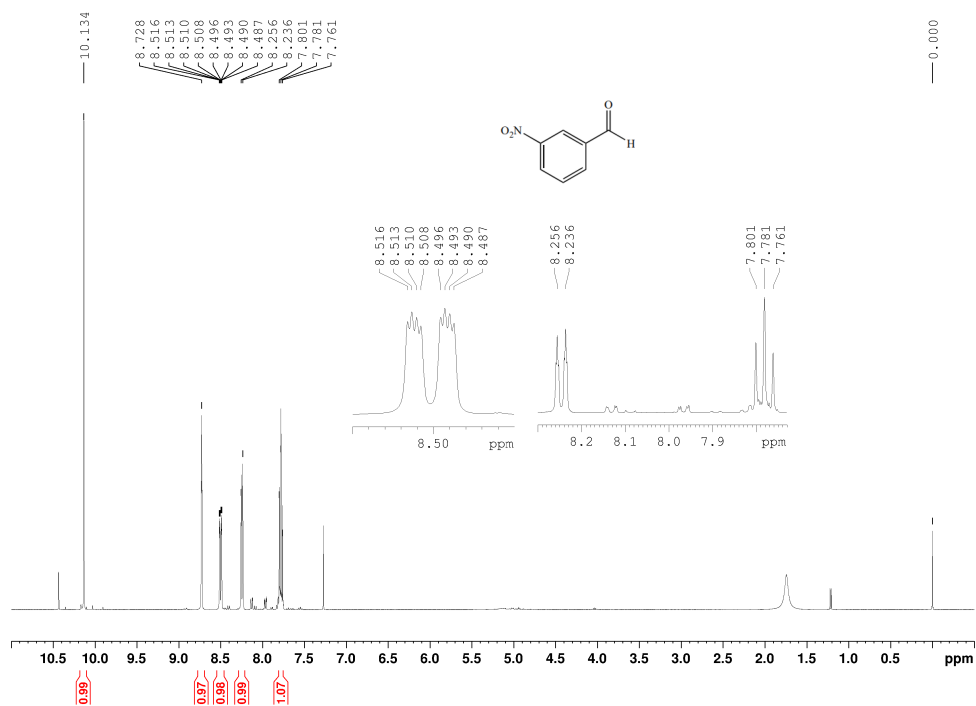


Figure 4: 3-nitrobenzaldehyde NMR

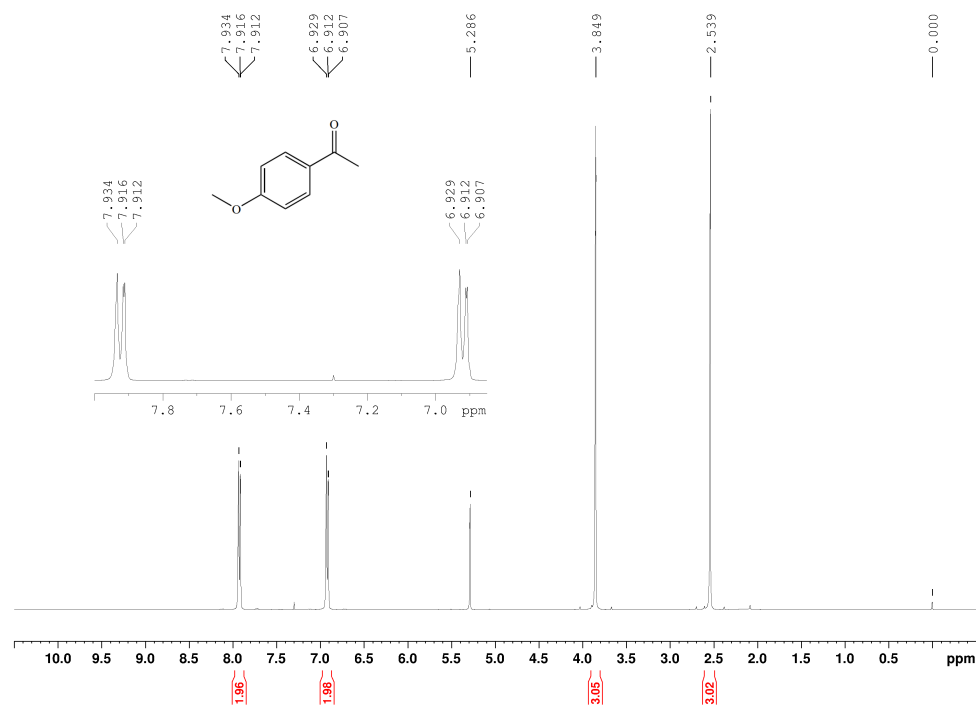


Figure 5: 1-(4-methoxyphenyl)ethan-1-one NMR

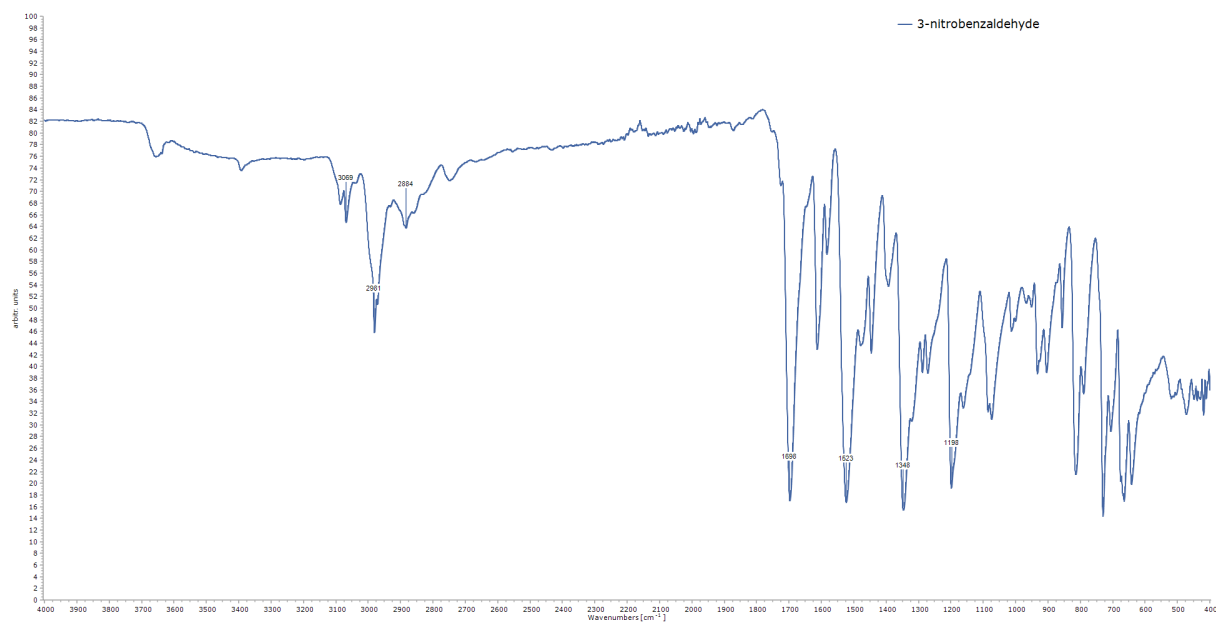


Figure 8: 3-nitrobenzaldehyde IR

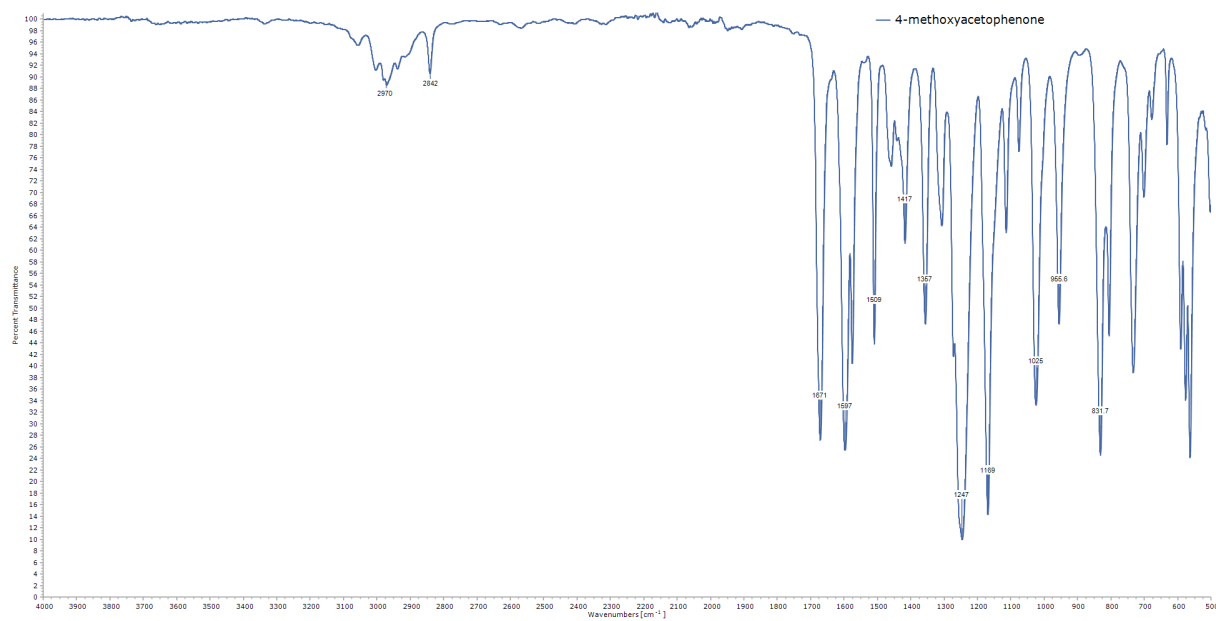


Figure 9: 1-(4-methoxyphenyl)ethan-1-one IR

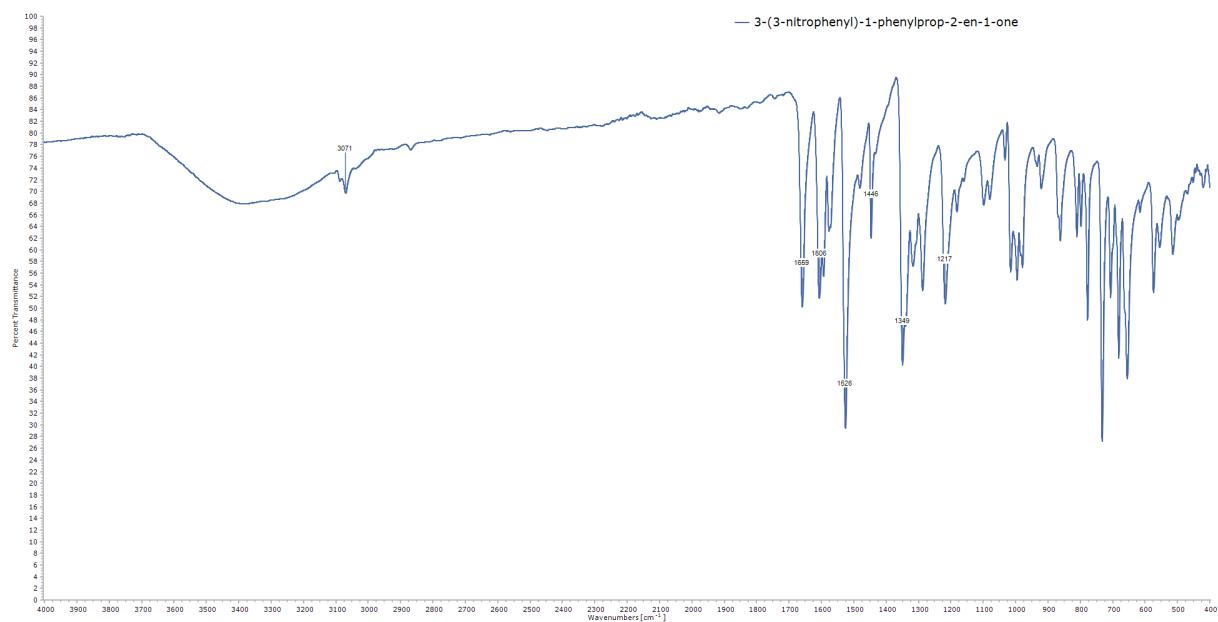


Figure 10: 3-(3-nitrophenyl)-1-phenylprop-2-en-1-one IR

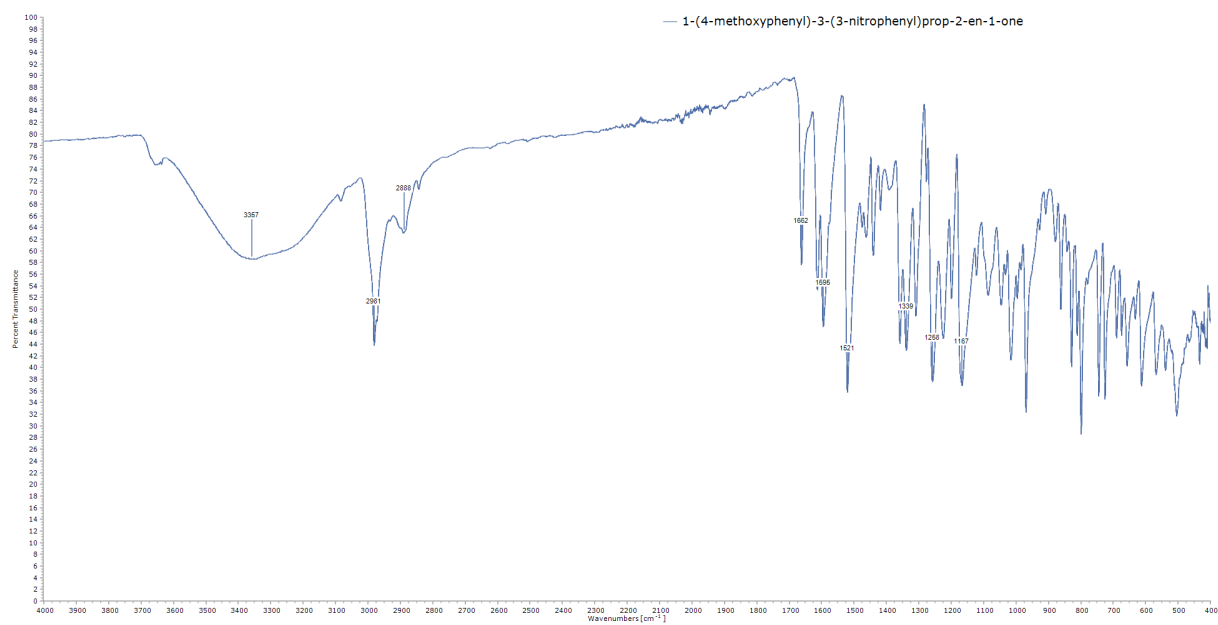


Figure 11: 1-(4-methoxyphenyl)-3-(3-nitrophenyl)prop-2-en-1-one IR

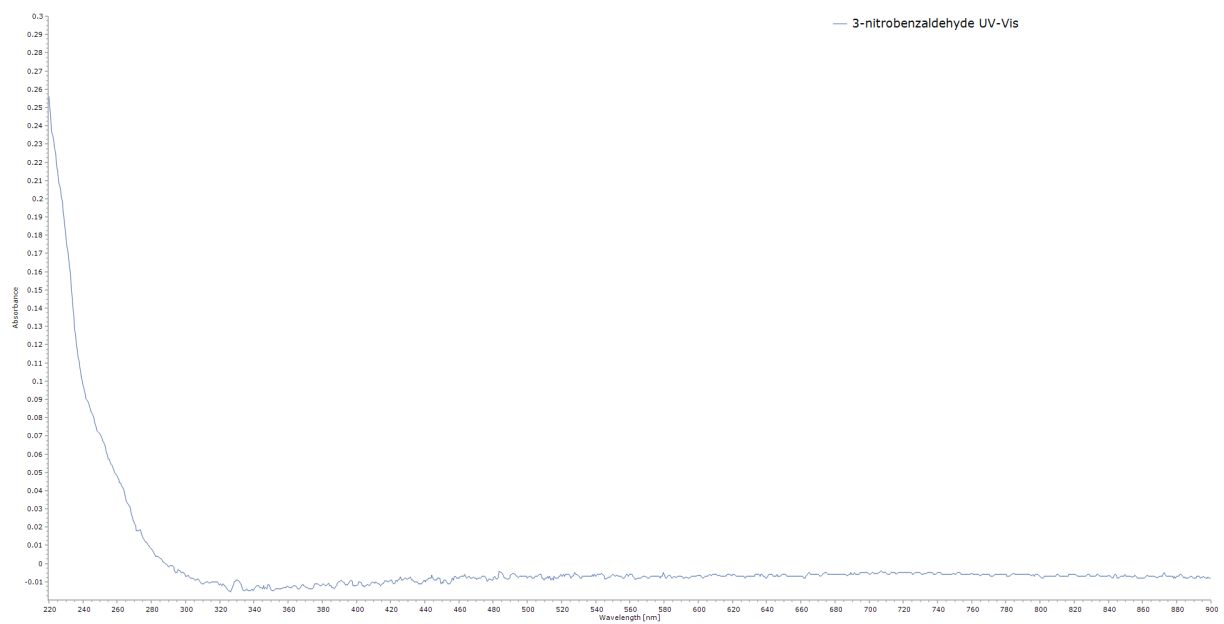


Figure 12: 3-nitrobenzaldehyde UV-Vis

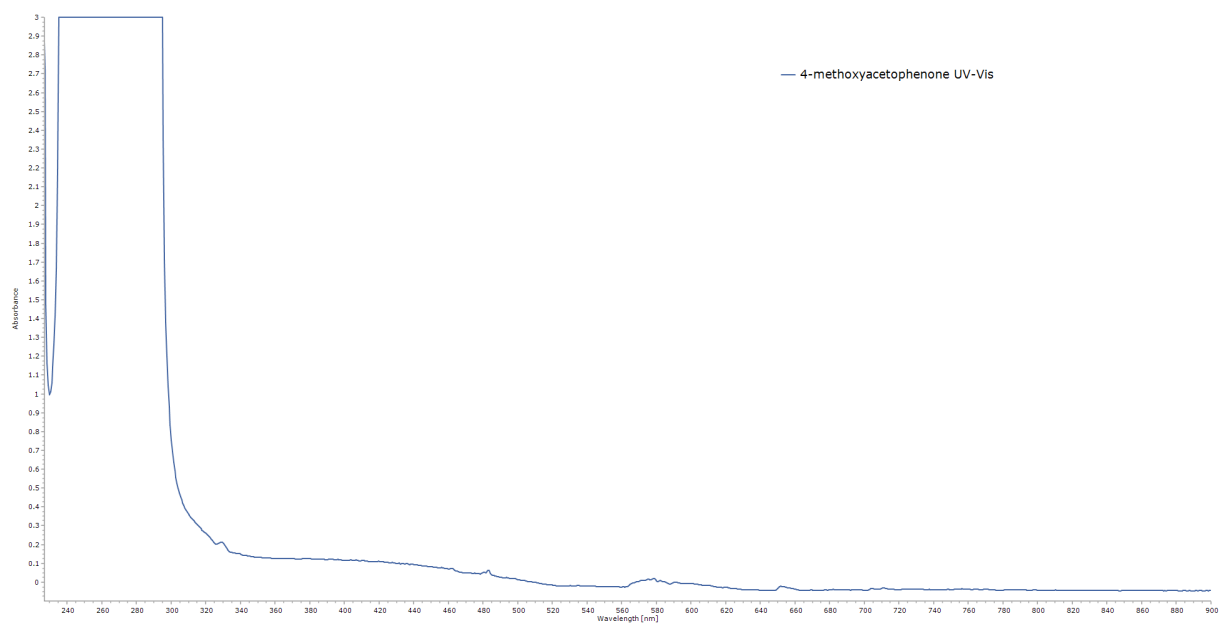


Figure 13: 1-(4-methoxyphenyl)ethan-1-one UV-Vis

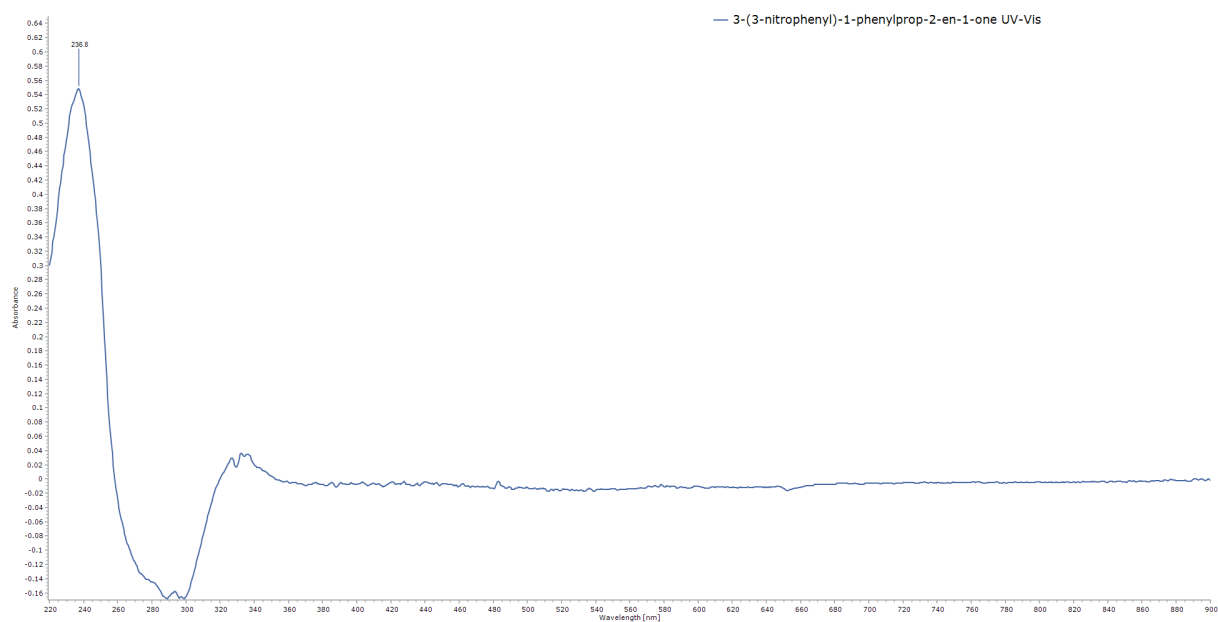


Figure 14: 3-(3-nitrophenyl)-1-phenylprop-2-en-1-one UV-Vis

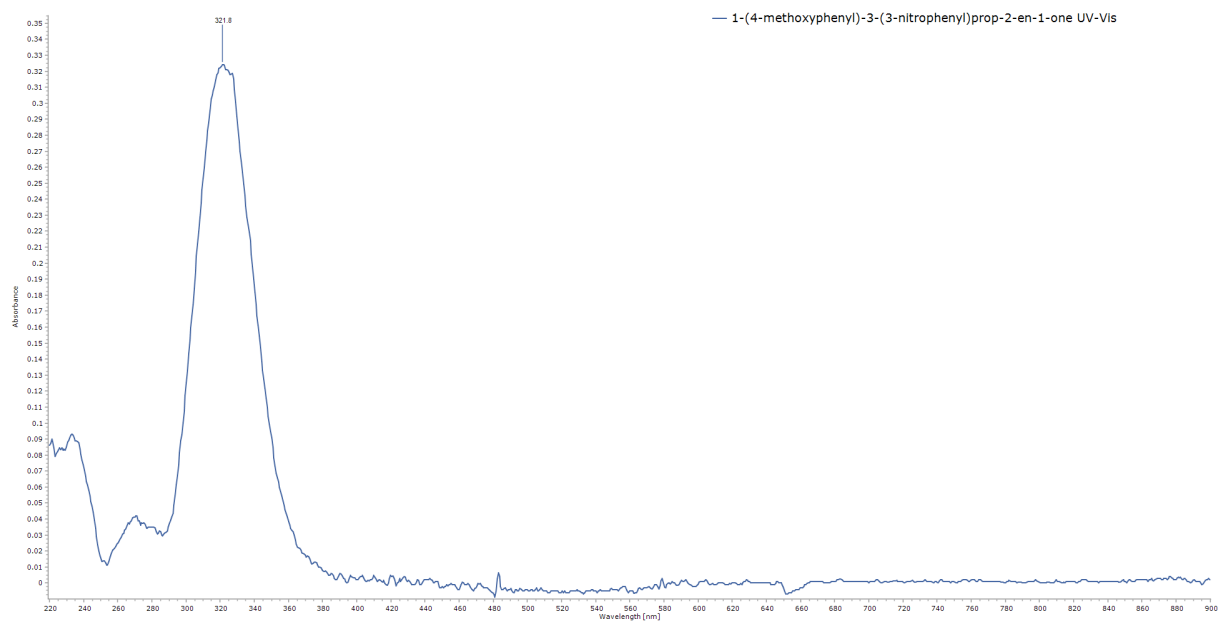


Figure 15: 1-(4-methoxyphenyl)-3-(3-nitrophenyl)prop-2-en-1-one UV-Vis

APPENDIX B: MECHANISMS

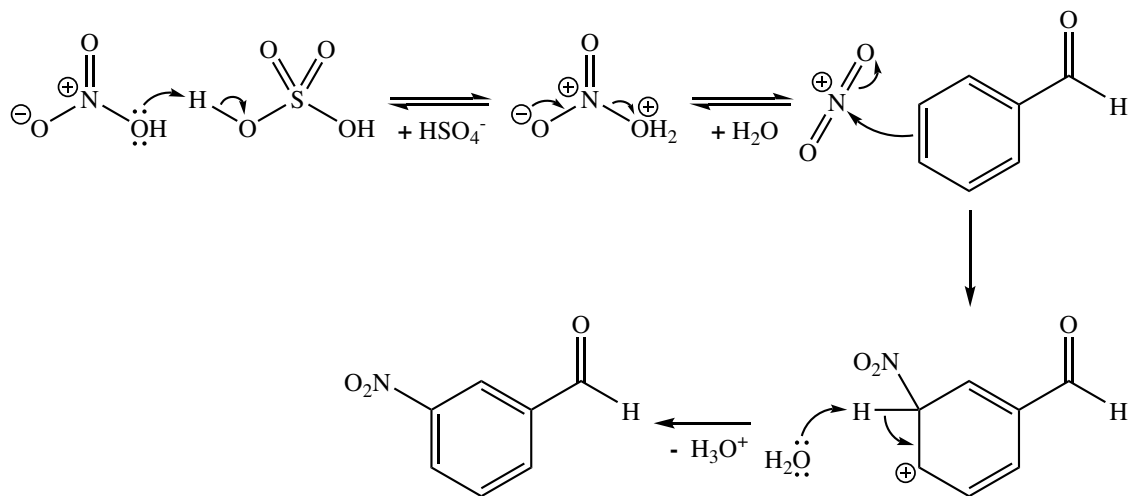


Figure 16: Mechanism of the nitration of benzaldehyde

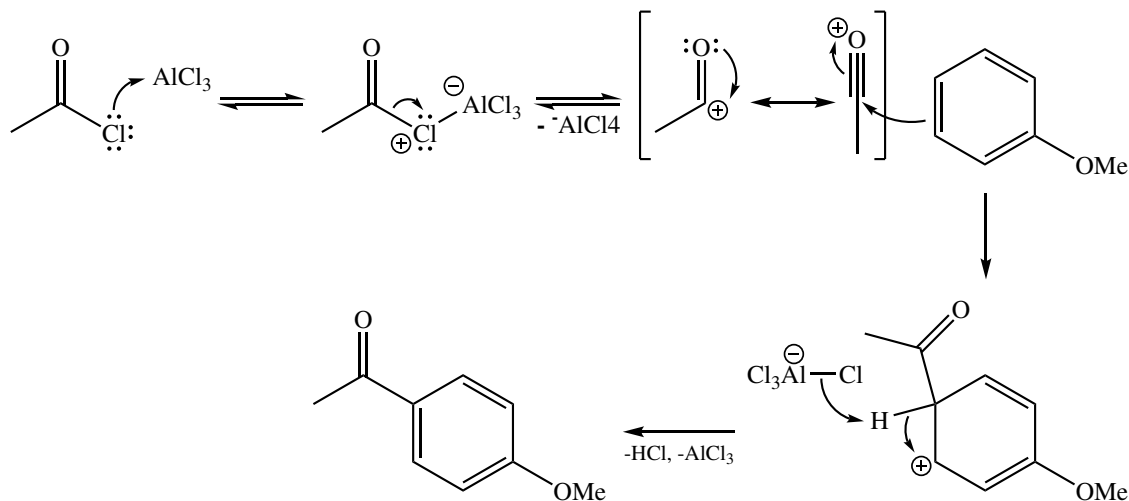


Figure 17: Mechanism of the acetylation of anisole

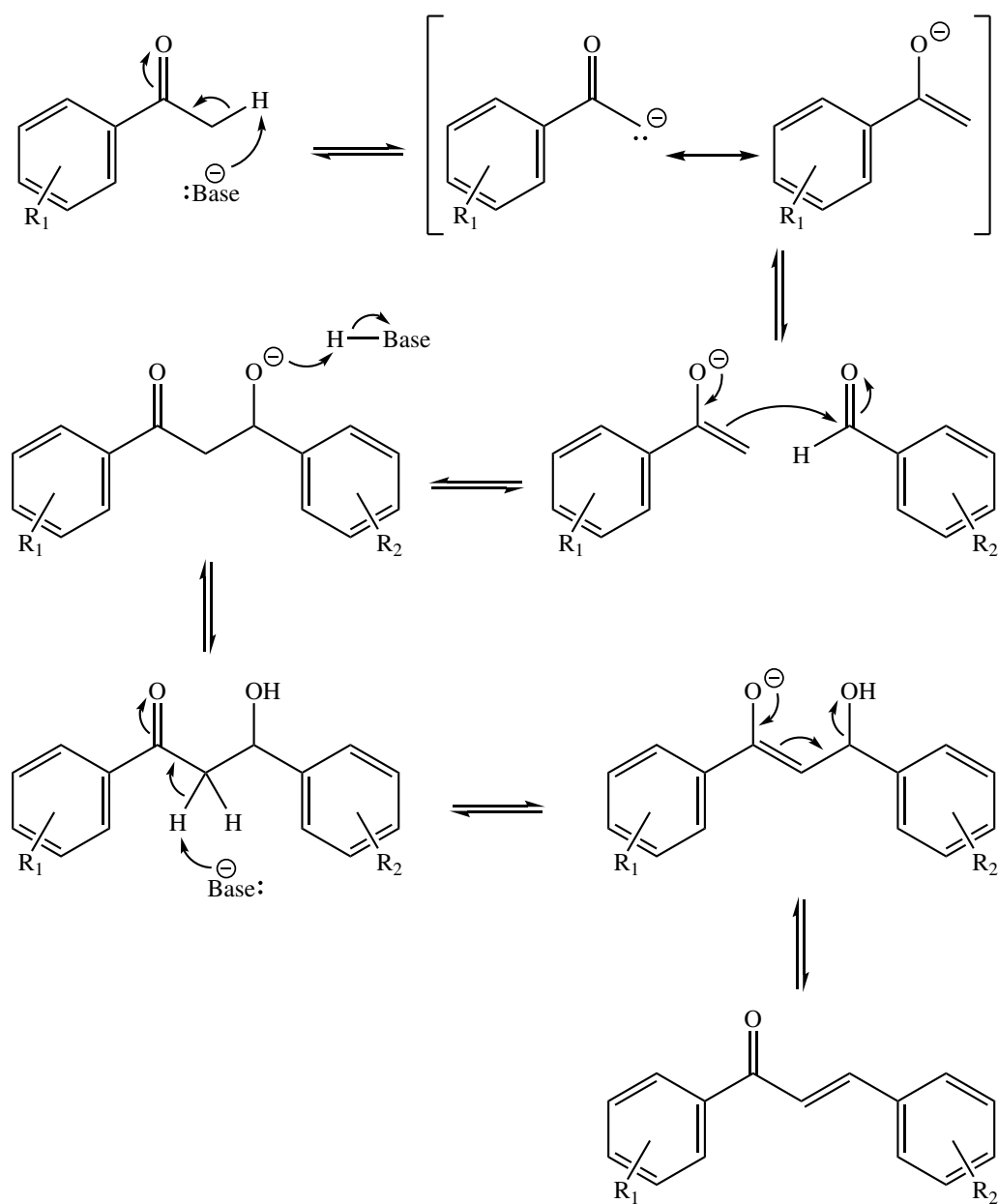


Figure 18: Mechanism of the formation of chalcone